






ORIGINAL ARTICLE

Radioimmunotherapy with an ^{211}At -labeled anti-tissue factor antibody protected by sodium ascorbate

Hiroki Takashima¹  | Yoshikatsu Koga^{1,2}  | Shino Manabe^{3,4,5}  | Kazunobu Ohnuki⁶ | Ryo Tsumura¹  | Takahiro Anzai¹ | Nozomi Iwata¹ | Yang Wang⁷ | Takuya Yokokita⁷ | Yukiko Komori⁷ | Daiki Mori⁷ | Sachiko Usuda⁷ | Hiromitsu Haba⁷ | Hirofumi Fujii⁶ | Yasuhiro Matsumura⁸ | Masahiro Yasunaga¹ 

¹Division of Developmental Therapeutics, Exploratory Oncology Research & Clinical Trial Center, National Cancer Center, Kashiwa, Japan

²Department of Strategic Programs, Exploratory Oncology Research & Clinical Trial Center, National Cancer Center, Kashiwa, Japan

³Laboratory of Functional Molecule Chemistry, Pharmaceutical Department and Institute of Medicinal Chemistry, Hoshi University, Tokyo, Japan

⁴Research Center for Pharmaceutical Development, Graduate School of Pharmaceutical Sciences & Faculty of Pharmaceutical Sciences, Tohoku University, Sendai, Japan

⁵Glycometabolic Biochemistry Laboratory, RIKEN, Wako, Japan

⁶Division of Functional Imaging, Exploratory Oncology Research & Clinical Trial Center, National Cancer Center, Kashiwa, Japan

⁷Nishina Center for Accelerator-Based Science, RIKEN, Wako, Japan

⁸Department of Immune Medicine, National Cancer Center Research Institute, National Cancer Center, Chuo-ku, Tokyo, Japan

Correspondence

Masahiro Yasunaga, Division of Developmental Therapeutics, Exploratory Oncology Research & Clinical Trial Center, National Cancer Center, 6-5-1 Kashiwanoha, Kashiwa, Chiba 277-8577, Japan.
Email: mayasuna@east.ncc.go.jp

Funding information

Japan Agency for Medical Research and Development (AMED), Grant/Award Number: 19cm0106237h0002; National Cancer Center Research and Development Fund, Grant/Award Number: 29-A-9, 30-S-4 and 2020-A-9; RIKEN Engineering Network Project; JSPS Grant-in-Aid for Scientific Research on Innovative Areas, Grant/Award Number: 16H06278

Abstract

Tissue factor (TF), the trigger protein of the extrinsic blood coagulation cascade, is abundantly expressed in various cancers including gastric cancer. Anti-TF monoclonal antibodies (mAbs) capable of targeting cancers have been successfully applied to armed antibodies such as antibody-drug conjugates (ADCs) and molecular imaging probes. We prepared an anti-TF mAb, clone 1084, labeled with astatine-211 (^{211}At), as a promising alpha emitter for cancer treatment. Alpha particles are characterized by high linear energy transfer and a range of 50–100 μm in tissue. Therefore, selective and efficient tumor accumulation of alpha emitters results in potent antitumor activities against cancer cells with minor effects on normal cells adjacent to the tumor. Although the ^{211}At -conjugated clone 1084 (^{211}At -anti-TF mAb) was disrupted by an ^{211}At -induced radiochemical reaction, we demonstrated that astatinated anti-TF mAbs eluted in 0.6% or 1.2% sodium ascorbate (SA) solution were protected from antibody denaturation, which contributed to the maintenance of cellular binding activities and cytotoxic effects of this immunoconjugate. Although body weight loss was observed in mice administered a 1.2% SA solution, the loss was transient and the radioprotectant seemed to be tolerable in vivo. In a high TF-expressing gastric cancer xenograft model, ^{211}At -anti-TF mAb in 1.2% SA exerted a significantly greater antitumor effect than nonprotected ^{211}At -anti-TF mAb. Moreover, the antitumor activities of the protected immunoconjugate in gastric cancer xenograft models were dependent on the

This is an open access article under the terms of the Creative Commons Attribution-NonCommercial-NoDerivs License, which permits use and distribution in any medium, provided the original work is properly cited, the use is non-commercial and no modifications or adaptations are made.

© 2021 The Authors. *Cancer Science* published by John Wiley & Sons Australia, Ltd on behalf of Japanese Cancer Association.

level of TF in cancer cells. These findings suggest the clinical availability of the radio-protectant and applicability of clone 1084 to ^{211}At -radioimmunotherapy.

KEYWORDS

antibody denaturation, astatine-211, radioimmunotherapy, sodium ascorbate, tissue factor

1 | INTRODUCTION

Gastric cancer remains one of the most common and deadliest cancers worldwide.¹ Although patients with metastatic gastric cancer have been managed by combination chemotherapeutic regimens, the efficacy of these regimens is not satisfactory.² In addition to cytotoxic agents, molecular targeted therapies for patients with cancer have been introduced to clinical practice. Trastuzumab, an anti-human epidermal growth factor receptor 2 (HER2) monoclonal antibody (mAb), is clinically available for patients with advanced gastric cancer.^{2,3} In addition to the naked mAb, increasing attention has been paid to the HER2-targeted antibody-drug conjugate (ADC), a mAb conjugated with cytotoxic agents.^{4,5} Although HER2-targeted therapies are beneficial and promising, their contributions are hampered by limited expression (up to 20%) of HER2 in gastric adenocarcinomas^{2,6} and resistance to HER2-targeted therapy.⁷ Therefore, it is assumed that the development of novel treatments targeting other molecules will provide benefits to patients with HER2-negative gastric cancer and in recurrence after HER2-targeted therapies.

Patients with malignancies including gastric cancer have a higher risk of venous thromboembolism compared with those with nonmalignant diseases.⁸ Tissue factor (TF), a 47-kDa transmembrane glycoprotein,⁹ triggers the extrinsic blood coagulation cascade and plays a physiological role in hemostasis. In pathological settings, TF is over-expressed in various cancers including gastric cancer^{10,11} and seems to cause abnormal blood coagulation in patients with cancer.^{12,13} TF is one of the attractive target molecules for cancer treatment with an armed antibody because various anti-TF mAbs have been successfully applied to ADC¹⁴⁻²¹ and its antibody-photosensitizer conjugate.²² Thus, we produced anti-TF mAbs for cancer targeting.^{16,19,22-29}

Alpha particles are characterized by high linear energy transfer (LET) resulting in efficient cell death via deoxyribonucleic acid (DNA) double-strand breaks. Moreover, alpha particles have a range of 50-100 μm in tissue, which is equivalent to 5-10 cells.³⁰ Therefore, selective and efficient tumor accumulation of alpha emitters results in potent antitumor activities with minor effects on normal cells adjacent to the tumor. Astatine-211 (^{211}At) is an alpha emitter with a half-life of 7.2 hours, which is long enough to permit the preparation and evaluation of ^{211}At -labeled radiopharmaceuticals.³¹ Due to the following favorable properties, the radionuclide is a promising alpha emitter for cancer treatment.³¹ First, high yields of ^{211}At produced by the cyclotron are sufficient to administer ^{211}At -labeled radiopharmaceuticals at clinically effective doses. Second, 100% of ^{211}At decays result in alpha emission. Lastly, in addition to alpha decay, ^{211}At emits characteristic X-rays that can be used for visualization

and quantification of its biodistribution by planar and single-photon emission computed tomography (SPECT).

In this study, we produced and prepared an astatinated mAb using an anti-TF mAb, clone 1084, and evaluated the immunconjugate. First, as ^{211}At disturbs the binding activity of antibodies in a radiation dose-dependent manner,^{32,33} we confirmed ^{211}At -induced antibody denaturation and investigated the radioprotective effects and in vivo tolerability of sodium ascorbate (SA), one of the free radical scavengers. Second, we evaluated the in vivo antitumor effects of ^{211}At -conjugated anti-TF mAb protected by SA in gastric cancer xenograft models.

2 | MATERIALS AND METHODS

2.1 | An anti-human TF mAb, clone 1084

Clone 1084 is a rat anti-human TF mAb established in our laboratory.¹⁹ In this study, we made a humanized anti-TF mAb by grafting the complementarity-determining region of clone 1084 into the human antibody scaffold.

2.2 | Gastric cancer cell lines

Human gastric cancer cell lines MKN-1, MKN-45, and NUGC-3 were purchased from the Japanese Collection of Research Bioresources (JCRB). The human gastric cancer cell line SH-10-TC and gastroesophageal junction cancer cell line OE19 were purchased from the RIKEN Bioresource Research Center (RIKEN BRC) and the European Collection of Authenticated Cell Cultures (ECACC), respectively. The human signet ring cell gastric cancer cell line 44As3 was provided by Dr K. Yanagihara (National Cancer Center).³⁴⁻³⁶ The cells were cultured in RPMI-1640 medium (FUJIFILM Wako Pure Chemical Corporation) supplemented with 10% fetal bovine serum (Thermo Fisher Scientific), 100 units/mL penicillin, 100 $\mu\text{g}/\text{mL}$ streptomycin, and 0.25 $\mu\text{g}/\text{mL}$ amphotericin B (FUJIFILM Wako Pure Chemical Corporation) at 37°C in a humidified 5% CO_2 atmosphere.

2.3 | TF expression

According to a protocol described previously, we determined TF expression on gastric cancer cell lines using clone 1084 as a primary antibody.²⁹

2.4 | ^{211}At production

^{211}At was produced in the $^{209}\text{Bi}(\alpha, 2n)^{211}\text{At}$ reaction by irradiating a metallic bismuth target with a 29.0-MeV alpha beam delivered from the RIKEN AVF cyclotron (RIKEN). Subsequently, ^{211}At was sublimated from the bismuth target and dissolved in chloroform. Then, the solvent was dried by N_2 gas at room temperature (RT) to obtain a solid ^{211}At .

2.5 | Preparation of ^{211}At -conjugated anti-TF mAb

N-[2-(maleimido)ethyl]-3-(trimethylstannyl)benzamide was prepared in two steps using a $\text{PdCl}_2(\text{PPh}_3)_2$ -catalyzed reaction.³⁷ Then, the maleimide portion was attached via the typical amide bond formation reaction using 1-(3-dimethylaminopropyl)-3-ethylcarbodiimide hydrochloride as a coupling reagent. *N*-[2-(maleimido)ethyl]-3-(trimethylstannyl)benzamide was dissolved in dimethyl sulfoxide and stored at -80°C until use.

N-[2-(maleimido)ethyl]-3-(trimethylstannyl)benzamide was attached to humanized clone 1084, as previously described (Figure 1).¹⁹ In this study, we adopted 15 mmol/L cysteamine hydrochloride (Sigma-Aldrich) to cleave the disulfide bonds in the antibody. The number of trimethylstannyl per antibody (Sn-antibody ratio) was determined as previously described.³⁸ Trimethylstannyl-conjugated clone 1084 (Sn-anti-TF mAb) was stored in phosphate-buffered saline (PBS) at -80°C until use.

We labeled Sn-anti-TF mAb with ^{211}At as previously described with minor modifications (Figure 1).^{39,40} In brief, by ultrafiltration, the

storage solution (PBS) was changed to PBS (pH 5.5), the pH of which was adjusted by adding 0.1 mol/L citric acid. For activating ^{211}At , a dry residue was dissolved in 0.04 mg/mL *N*-chlorosuccinimide (NCS; TCI) in methanol/1% acetic acid. Then, ^{211}At (100 MBq/60 μL) was added to Sn-anti-TF mAb solution (100 μg /600 μL), and the mixture was agitated for 1 minute at RT. To exchange any remaining stannyl groups on the astatinated antibody to chloride, 2 mg/mL NCS in methanol/1% acetic acid (3 μL) was added to the mixture and agitated for 1 minute at RT. The reaction was quenched by adding 5 μL of 0.1 mol/L L-ascorbic acid (TCI) in water. After agitation for 5 minutes at RT, the astatinated anti-TF mAb was purified in PBS with or without SA (FUJIFILM Wako Pure Chemical Corporation) by size-exclusion chromatography on a PD-10 column (GE Healthcare) (Figure 1).

In this study, we labeled anti-TF mAbs with ^{211}At at RIKEN, and transferred the astatinated mAbs to the National Cancer Center (NCC) and evaluated the immunoconjugates. Radioactivity was measured using a germanium semiconductor detector (GEM P-type or GMX N-type; ORTEC) at RIKEN and a curie-meter (IGC-8; HITACHI) at NCC.

2.6 | Radiochemical yield and purity

Radiochemical yield was calculated by dividing the radioactivity of ^{211}At -conjugated anti-TF monoclonal antibody (^{211}At -anti-TF mAb) fractions by the initially applied radioactivity (100 MBq). Ultrafiltration analysis was performed to determine the radiochemical purity of ^{211}At -anti-TF mAbs. A total of 5 μL of the

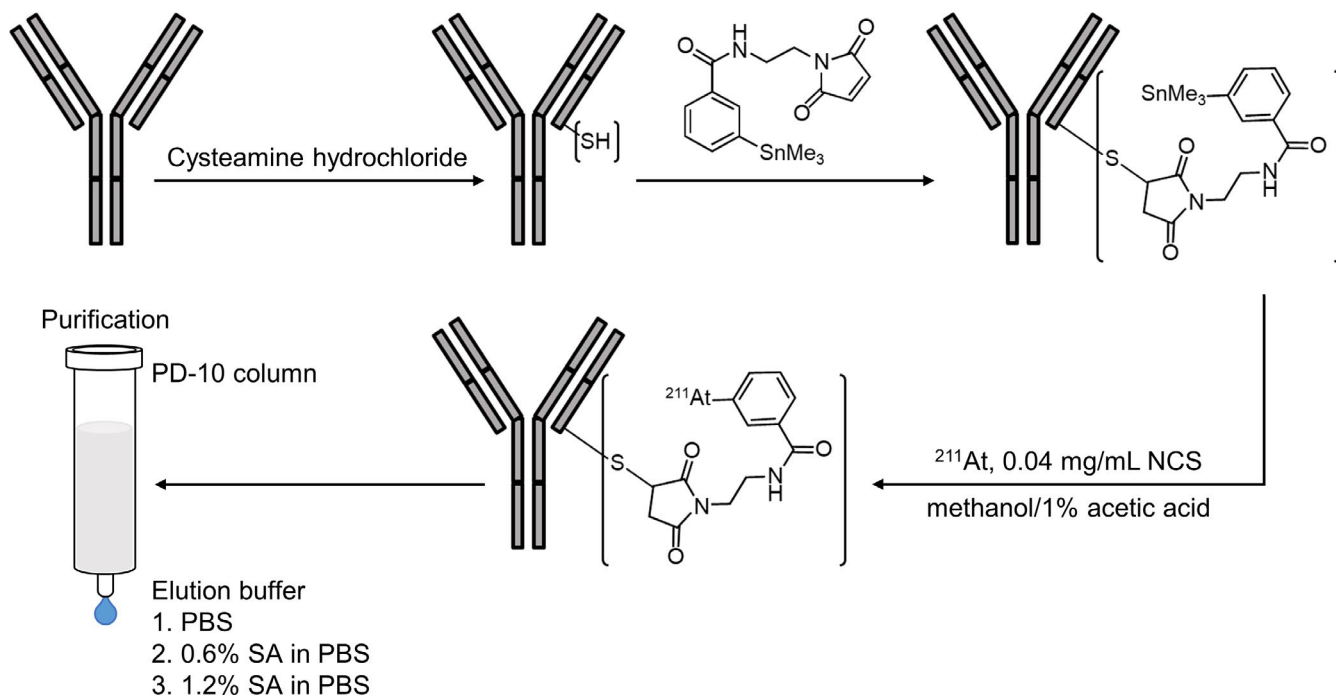


FIGURE 1 Preparation of astatine-211-conjugated anti-tissue factor monoclonal antibody (^{211}At -anti-TF mAb). This diagram shows the preparation of trimethylstannyl-conjugated anti-TF mAb and ^{211}At labeling. ^{211}At -conjugated anti-TF mAb was purified in phosphate-buffered saline (PBS) with or without sodium ascorbate (SA) by size-exclusion chromatography

astatinated anti-TF mAbs was added to 495 μL of their elution buffers. Free ^{211}At dissolved in PBS, 0.6% SA in PBS, or 1.2% SA in PBS, the radioactivities of which were equal to the corresponding immunoconjugates, was added to each of the dissolving buffers to achieve a final volume of 500 μL . Then, the samples were applied to the Amicon Ultra centrifugal filter unit with a molecular weight cutoff of 30 K (Merck KGaA) and centrifuged for 20 minutes at 14 000 g . The initial radioactivity and the radioactivity of flow through were measured using a gamma counter (2480 Wizard²; PerkinElmer). The radiochemical purity was calculated by the following formula: radiochemical purity = $(R_{\text{initial}} - R_{\text{flow through}} / \text{FT}_{\text{At-211}}) / R_{\text{initial}} \times 100$, where R is radioactivity and $\text{FT}_{\text{At-211}}$ is calculated by dividing the radioactivity of flow through in free ^{211}At samples dissolved in the corresponding buffer by the initial radioactivity. In addition to the ultrafiltration analysis, we validated the radiochemical purity by protein precipitation with methanol as previously described.⁴⁰

2.7 | Sodium dodecyl sulfate-polyacrylamide gel electrophoresis

We performed SDS-PAGE analysis on the day after ^{211}At labeling. After denaturation by heating at 95°C for 5 minutes, 0.2 μg of humanized clone 1084, 0.2 μg of Sn-anti-TF mAb, and 10 kBq of ^{211}At -anti-TF mAbs were electrophoresed in a 4%-15% gradient polyacrylamide gel (Bio-Rad Laboratories). Then, the gel was fixed in a 50% methanol/5% acetic acid solution for 20 minutes. The fixed gel was exposed to an imaging plate (FUJIFILM), and the exposed plate was read with an imaging plate reader (FLA-7000; FUJIFILM). After autoradiography, antibodies in the gel were visualized using the silver staining kit (FUJIFILM Wako Pure Chemical Corporation).

2.8 | Binding activity

2.8.1 | Experiment 1

44As3 and OE19 cells were harvested in enzyme-free cell dissociation buffer (Thermo Fisher Scientific) and suspended in PBS with 0.1% bovine serum albumin (BSA) and 2 mmol/L ethylenediaminetetraacetic acid (EDTA) (BE-PBS). Then, 2×10^5 cells were incubated for 30 minutes on ice with 5 $\mu\text{g}/\text{mL}$ of humanized clone 1084, Sn-anti-TF mAb, or ^{211}At -anti-TF mAbs. After washing with BE-PBS, the cells were incubated for 30 minutes on ice with 5 $\mu\text{g}/\text{mL}$ of Alexa Fluor 647-conjugated goat polyclonal anti-human immunoglobulin antibody (Thermo Fisher Scientific). Subsequently, the cells were washed with BE-PBS and the nuclei were stained with propidium iodide (PI; Thermo Fisher Scientific). The samples were run on a SH800S Cell Sorter (Sony), and the acquired data were analyzed using the FlowJo 7.6.5 software (Becton, Dickinson and

Company). The flow cytometry analysis was performed 7 days after ^{211}At labeling.

2.8.2 | Experiment 2

Similarly, the cells were nonenzymatically harvested and suspended in BE-PBS. Aliquots of 2×10^5 cells were incubated for 30 minutes on ice with 10 kBq of ^{211}At -anti-TF mAbs, and then, samples were washed three times with BE-PBS. The radioactivity bound to the cells was measured using a gamma counter (PerkinElmer). The percentage of cellular binding was calculated by dividing the radioactivity bound to the cells by the initially added radioactivity. The cellular binding activities were determined at 6 hours after ^{211}At labeling.

2.9 | Cytocidal effect

A total of 2×10^3 44As3 cells, 3×10^3 NUGC-3 cells, 1×10^3 MKN-1 cells, 2×10^3 SH-10-TC cells, 2×10^3 MKN-45 cells, or 7×10^3 OE19 cells were plated on 96-well plates (Corning) and cultured overnight. Then, the growth medium was replaced with a medium containing serially diluted free ^{211}At or ^{211}At -anti-TF mAbs, and the cells were incubated for 120 hours at 37°C. Cell viabilities were determined using the Cell Counting Kit-8 (Dojindo).

2.10 | Animal models

The animal experiment was approved by the Committees for Animal Experimentation of the National Cancer Center, Japan. All animal procedures were performed in compliance with the Guidelines for the Care and Use of Experimental Animals established by the Committees. These guidelines meet the ethical standards required by law and also comply with the guidelines for the use of experimental animals in Japan.

A total of 5×10^5 44As3 cells, 5×10^6 MKN-45 cells, or 3×10^6 OE19 cells suspended in 100 μL of PBS were inoculated into the flank region of 5-week-old female BALB/c nu/nu mice (Charles River Japan). Tumor volume was calculated by the following formula: tumor volume = $(\text{length} \times \text{width}^2) \times 1/2$.

2.11 | Toxicity of free ^{211}At and ^{211}At -conjugated anti-TF mAb

Nine-week-old female BALB/c nu/nu mice (Charles River Japan) were intravenously administered 1.2% SA in PBS, 0.1-2 MBq of free ^{211}At , or ^{211}At -anti-TF mAb in PBS containing 1.2% SA. After administration, body weight was measured once every 2 days. For humane reasons, mice in which body weight loss exceeded 20% were euthanized.

2.12 | In vivo antitumor effect

2.12.1 | Experiment 1

When the tumor volume of 44As3 subcutaneous tumors reached approximately 160 mm³, the model mice were randomly divided into four groups and intravenously administered PBS, 1.2% SA in PBS, 1 MBq of ²¹¹At-anti-TF mAb eluted in PBS, or 1 MBq of ²¹¹At-anti-TF mAb eluted in PBS containing 1.2% SA. Tumor volume and body weight were measured once every 2 days.

2.12.2 | Experiment 2

When the tumor volume of 44As3, MKN-45, and OE19 subcutaneous tumors reached approximately 250 mm³, 280 mm³, and 300 mm³, respectively, the model mice were randomly divided into two groups and intravenously administered 1.2% SA in PBS or 1 MBq of ²¹¹At-anti-TF mAb eluted in PBS containing 1.2% SA. Tumor volume and body weight were measured once every 2 days. Tumor progression was defined as tumor volume greater than 800 mm³.⁴¹

2.13 | Statistical analysis

Repeated-measures ANOVA followed by the Tukey post hoc test were used to analyze tumor volume in model mice bearing 44As3 subcutaneous tumors administered PBS, 1.2% SA in PBS, 1 MBq of ²¹¹At-anti-TF mAb in PBS, or 1 MBq of ²¹¹At-anti-TF mAb in 1.2% SA. The Kaplan-Meier method was used to analyze progression-free survival. Statistical analyses were carried out with SPSS Statistics Version 18 (SPSS), and *P* < .05 was considered statistically significant.

3 | RESULTS

3.1 | TF expression

TF expression on the cell membrane of gastric cancer cells was determined by flow cytometry. The numbers of TF molecules on 44As3, NUGC-3, MKN-1, SH-10-TC, MKN-45, and OE19 were 1 308 102, 658 587, 535 484, 470 635, 357 661, and 11 632 molecules per cell, respectively (Figure 2). Therefore, we used 44As3, NUGC-3, MKN-1,

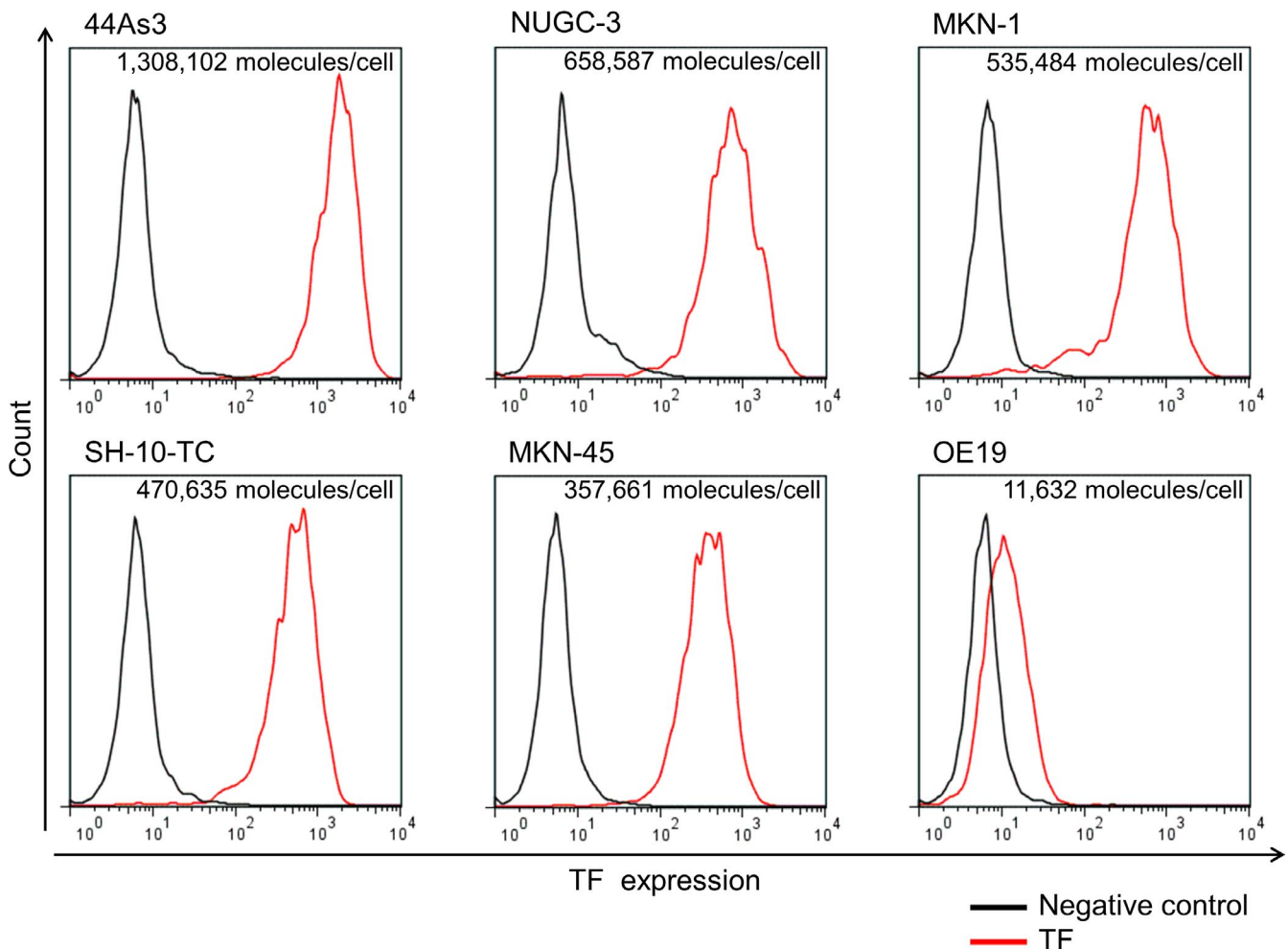


FIGURE 2 Tissue factor (TF) expression on the gastric cancer cell lines. The numbers of TF molecules on 44As3, NUGC-3, MKN-1, SH-10-TC, MKN-45, and OE19 were 1 308 102, 658 587, 535 484, 470 635, 357 661, and 11 632 molecules per cell, respectively

SH-10-TC, and MKN-45 as cell lines with high TF expression and OE19 as a cell line with low TF expression.

3.2 | ^{211}At -conjugated anti-TF mAb

The Sn-antibody ratio was 1.78. Radiochemical yields of ^{211}At -anti-TF mAb in PBS, 0.6% SA, and 1.2% SA were 20%-41%, 29%-37%, and 29%-54%, respectively. Ultrafiltration analysis-based radiochemical purity of the immunoconjugates in PBS, 0.6% SA, and 1.2% SA was 96%. Radiochemical purities determined by protein precipitation analysis in PBS, 0.6% SA, and 1.2% SA were 96%, 97%, and 97%, respectively.

3.3 | ^{211}At -induced antibody denaturation and radioprotective effects of SA

In the SDS-PAGE analysis, ^{211}At -anti-TF mAbs in 0.6% and 1.2% SA visualized by silver staining yielded band patterns, which were similar to Sn-anti-TF mAb (Figure 3). In contrast, ^{211}At -anti-TF mAb in PBS was smeared (Figure 3). In the autoradiogram of the gel, similarly, the astatinated mAbs in PBS and SA solutions were visualized as smear and band patterns, respectively (Figure 3). These findings suggest that ^{211}At -anti-TF mAb in PBS was disrupted by the radionuclide, and 0.6% and 1.2% SA protected the immunoconjugates from antibody denaturation. Consistently, flow cytometry analysis revealed that the binding activity of the astatinated mAb in PBS was disturbed compared with anti-TF mAb and Sn-anti-TF mAb (Figure 4A). On the other hand, ^{211}At -anti-TF mAbs in 0.6% and 1.2% SA, as well as the naked mAb and Sn-anti-TF mAb, bound to cancer cells based on the level of TF

on the cell membrane (Figures 2 and 4A; Figure S2). Similarly, the percentages of anti-TF mAbs in PBS, 0.6% SA, and 1.2% SA bound to 44As3 cells were $2.67 \pm 0.40\%$, $20.66 \pm 0.80\%$, and $17.52 \pm 3.58\%$, respectively, and those bound to OE19 cells were $1.40 \pm 0.18\%$, $2.13 \pm 0.14\%$, and $1.97 \pm 0.09\%$, respectively (Figure 4B).

3.4 | Cytocidal effect

^{211}At -anti-TF mAb more efficiently killed 44As3 cells with high TF expression than free ^{211}At , whereas the cytocidal effect of the immunoconjugate on OE19 cells with low TF expression was comparable to that of free ^{211}At (Figure 5A). The astatinated anti-TF mAbs in 0.6% and 1.2% SA exerted greater cytotoxic effects on 44As3 cells than the astatinated mAb in PBS (Figure 5A). The cytotoxic effects of ^{211}At -anti-TF mAb in 1.2% SA on high TF-expressing 44As3, NUGC-3, MKN-1, SH-10-TC, and MKN-45 cells were greater than the effect on low TF-expressing OE19 cells, whereas the cytotoxic effects of free ^{211}At dissolved in 1.2% SA against these cancer cells were comparable (Figures 2 and 5B).

3.5 | Toxicity of 1.2% SA, free ^{211}At , and ^{211}At -conjugated anti-TF mAb

Although relative body weight loss reached $5.65 \pm 1.39\%$ at 2 days after administration of 1.2% SA in PBS, the loss was transient (Figure 6).

Body weight loss after administration of ^{211}At -anti-TF mAb in 1.2% SA was less than the corresponding dose of free ^{211}At (Figure 6).

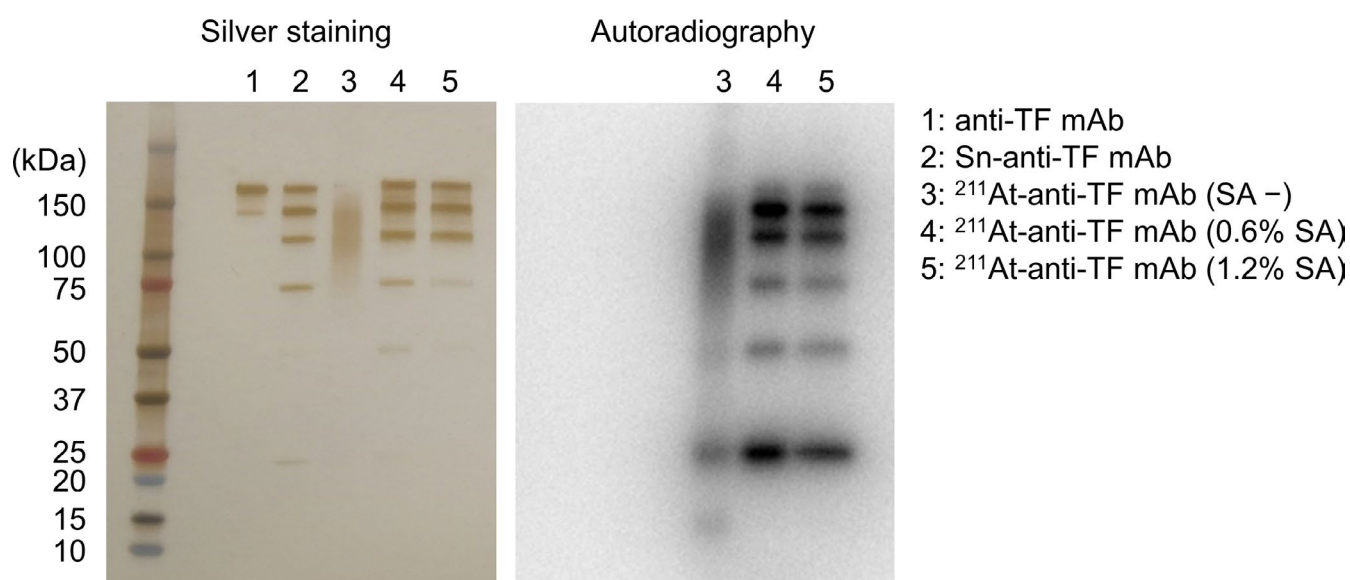


FIGURE 3 Astatine-211 (^{211}At)-induced antibody denaturation and radioprotective effects of sodium ascorbate (SA) determined by sodium dodecyl sulfate-polyacrylamide gel electrophoresis (SDS-PAGE) analysis

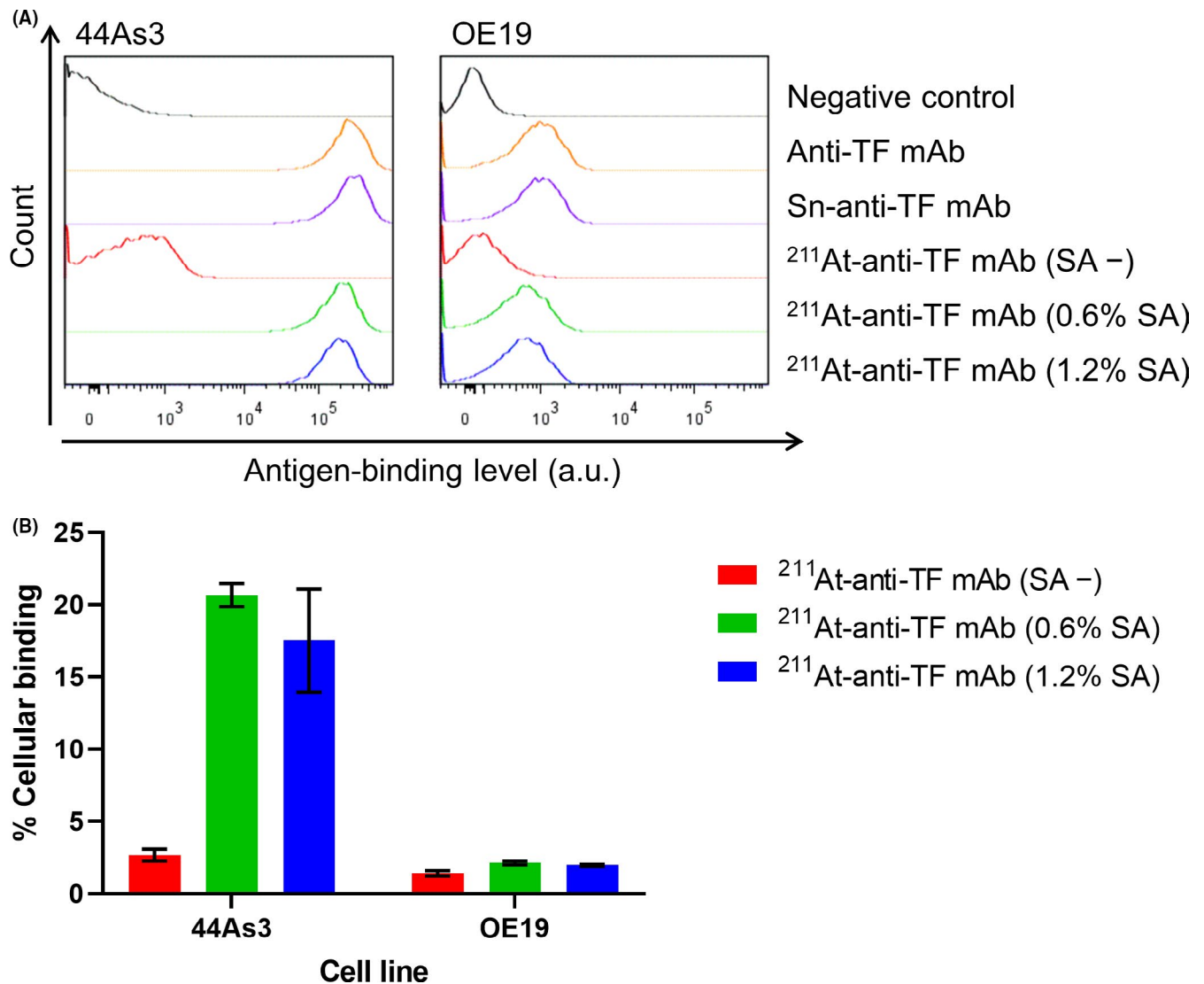


FIGURE 4 Binding activity. A, Flow cytometry analysis. B, The percentage of cellular binding. $N = 3$. Data are shown as means \pm standard deviation

3.6 | In vivo antitumor effect

In the 44As3 xenograft model with high TF expression, ^{211}At -anti-TF mAb eluted in PBS containing 1.2% SA exerted a significantly greater antitumor effect than the astatinated anti-TF mAb in PBS (Figure 7A; $P = .0045$). Body weight loss in model mice administered ^{211}At -anti-TF mAb in 1.2% SA was transient and comparable to that after administration of the immunoconjugate in PBS (Figure 7A). Compared with 1.2% SA in PBS, ^{211}At -anti-TF mAb significantly delayed tumor growth in 44As3, MKN-45, and OE19 xenograft models (Figure 7B; P -value: 44As3, $P = .0005$; MKN-45, $P = .0021$; OE19, $P = .0042$). In the 44As3 xenograft model with high TF expression, the median progression-free survival of groups treated with 1.2% SA in PBS and ^{211}At -anti-TF mAb eluted in 1.2% SA was 8 and 34 days, respectively (Figure 7B). In the high TF-expressing MKN-45 xenograft model, the median progression-free survival of groups treated with 1.2% SA and the astatinated anti-TF mAb was 8 and 30 days, respectively (Figure 7B). On the other hand, in the OE19 xenograft

model with low TF expression, the median progression-free survival of groups treated with 1.2% SA and ^{211}At -anti-TF mAb was 6 and 14 days, respectively (Figure 7B). Body weight loss after administration of the immunoconjugate was transient (Figure 7B).

4 | DISCUSSION

As there was concern that the ^{211}At -induced radiochemical reaction disturbed the binding activity of mAbs,^{32,33} we evaluated whether ^{211}At -anti-TF mAb was denatured. In the SDS-PAGE analysis, ^{211}At -anti-TF mAb eluted in PBS was smeared, in contrast to Sn-anti-TF mAb (Figure 3). These findings suggest that the astatinated anti-TF mAb in PBS was disrupted by the radionuclide. Similarly, the affinity of ^{211}At -anti-TF mAb in PBS for TF on the cancer cell surface was disturbed (Figure 4A,B).

McDevitt et al reported that L-ascorbic acid, a radioprotectant, improved the radiochemical recovery yield of a mAb labeled with

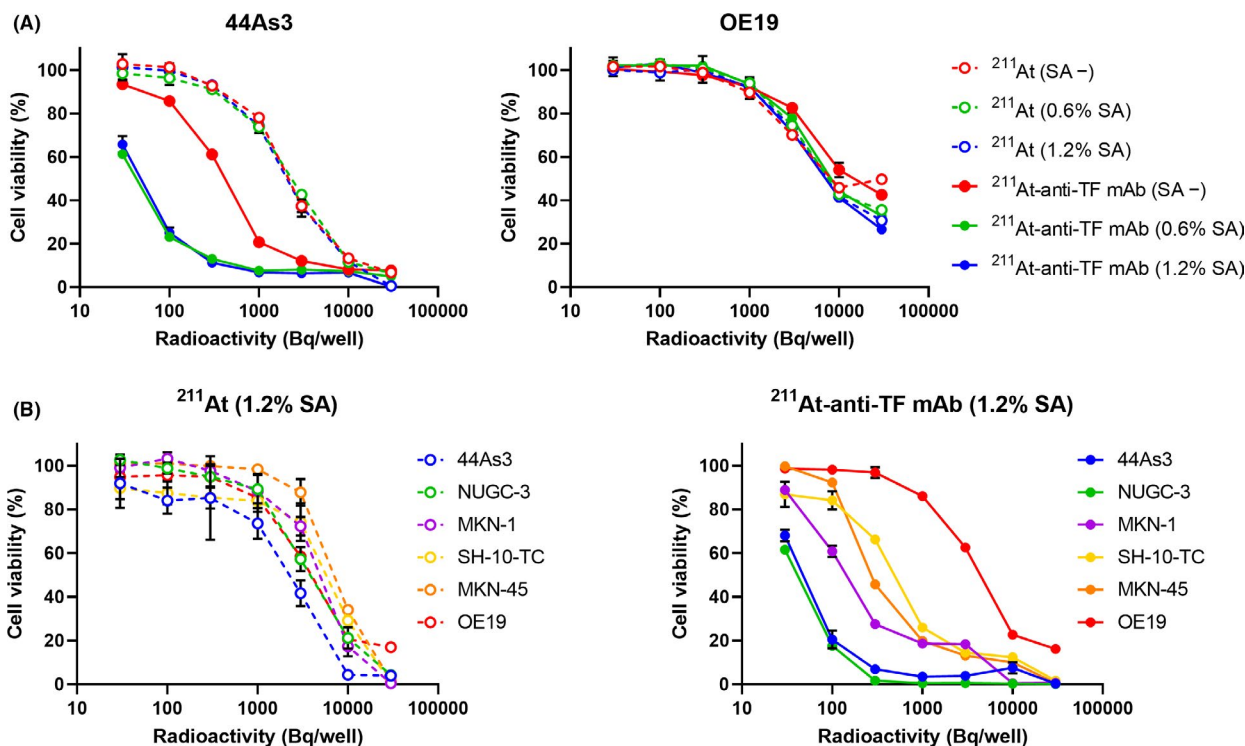


FIGURE 5 Cytocidal effect. A, The radioprotective effect of sodium ascorbate (SA) on cytotoxic effects of astatine-211-conjugated anti-tissue factor monoclonal antibody (^{211}At -anti-TF mAb). $N = 4$. Points, mean; bars, standard deviation. B, Cytotoxic effects of ^{211}At -anti-TF mAb in 1.2% SA is dependent on the level of TF in cancer cells. $N = 4$. Points, mean; bars, standard deviation

bismuth-213 (^{213}Bi), an alpha emitter, by avoiding ^{213}Bi -induced antibody denaturation.⁴² In this study, considering the pH of PBS containing a radioprotectant, we used SA for protecting ^{211}At -anti-TF mAb rather than L-ascorbic acid. Prior to preparing the astatinated anti-TF mAb eluted in PBS containing SA, we evaluated the cytotoxicity of SA itself against 44As3 cells in the presence of ^{211}At . In contrast to 0.6% or 1.2% SA, 2.4% SA showed cytotoxicity (Figure S1A-C). Therefore, we decided to elute ^{211}At -anti-TF mAbs in PBS containing 0%-1.2% SA, which did not hinder the evaluation of the antitumor activity exerted by the astatinated mAb itself. In the SDS-PAGE analysis, ^{211}At -anti-TF mAbs in PBS containing 0.6% and 1.2% SA as well as Sn-anti-TF mAb yielded band patterns, in contrast to a smear pattern of the astatinated anti-TF mAb in PBS (Figure 3). Consistently, the cellular binding activities of ^{111}In -anti-TF mAbs in 0.6% and 1.2% SA were maintained and comparable to the naked antibody (Figure 4A; Figure S2). These findings suggest that the radioprotective activity of SA resulted in maintaining the affinity of the astatinated mAb. Moreover, the protectant contributed to the cytotoxic effects of ^{211}At -anti-TF mAb, because the astatinated mAbs in 0.6% and 1.2% SA exerted greater cytotoxic effects on TF-overexpressing 44As3 cells than the immunoconjugate in PBS (Figure 5A).

Body weight loss after administration of PBS containing 1.2% SA was minimal and transient (Figure 6). Therefore, SA appears to protect the astatinated anti-TF mAb from ^{211}At -induced antibody denaturation without intolerable side effects (Figures 3, 4A,B and

6). On the other hand, body weight loss after administration of ^{211}At -anti-TF mAb in PBS containing 1.2% SA was less than the corresponding dose of free ^{211}At in the SA solution (Figure 6). ^{211}At of the immunoconjugate may be the main cause of body weight loss because noticeable body weight loss was not observed in mice intravenously administered 10 mg/kg naked anti-TF mAb.⁴³ Based on this toxicity test, 2.0 MBq of ^{211}At -anti-TF mAb in 1.2% SA seems to be the maximum tolerated dose (MTD) because the maximum percentage of body weight loss after administration was 19.8%. The toxicity profile of ^{211}At -conjugated anti-TF mAb is comparable to other astatinated antibodies. Li et al observed body weight loss in BALB/c nude mice intravenously administered 1.85 MBq of ^{211}At -labeled anti-frizzled homolog 10 antibody.⁴⁴ Although body weight loss reached approximately 10%-20% after administration, the loss was transient and 1.85 MBq of the immunoconjugate was tolerable. In another study, Robinson et al demonstrated that 1.665 MBq of ^{211}At -conjugated diabodies was close to the acute MTD in BALB/c nude mice based on body weight loss after administration.⁴⁵

As various anti-TF mAbs have been successfully applied to ADC,¹⁴⁻²¹ an antibody-photosensitizer conjugate,²² and a molecular imaging probe,^{24,27,28,46,47} TF is one of the attractive molecules for cancer targeting. In this study, we succeeded in preparing an anti-TF mAb labeled with ^{211}At . Alpha emitters such as ^{211}At efficiently induce cell death via DNA double-strand breaks,^{48,49} which is different from the cytotoxic mechanisms of drugs¹⁴⁻²¹ or photosensitizers²² conjugated to anti-TF mAbs. Thus, the astatinated anti-TF mAb is a

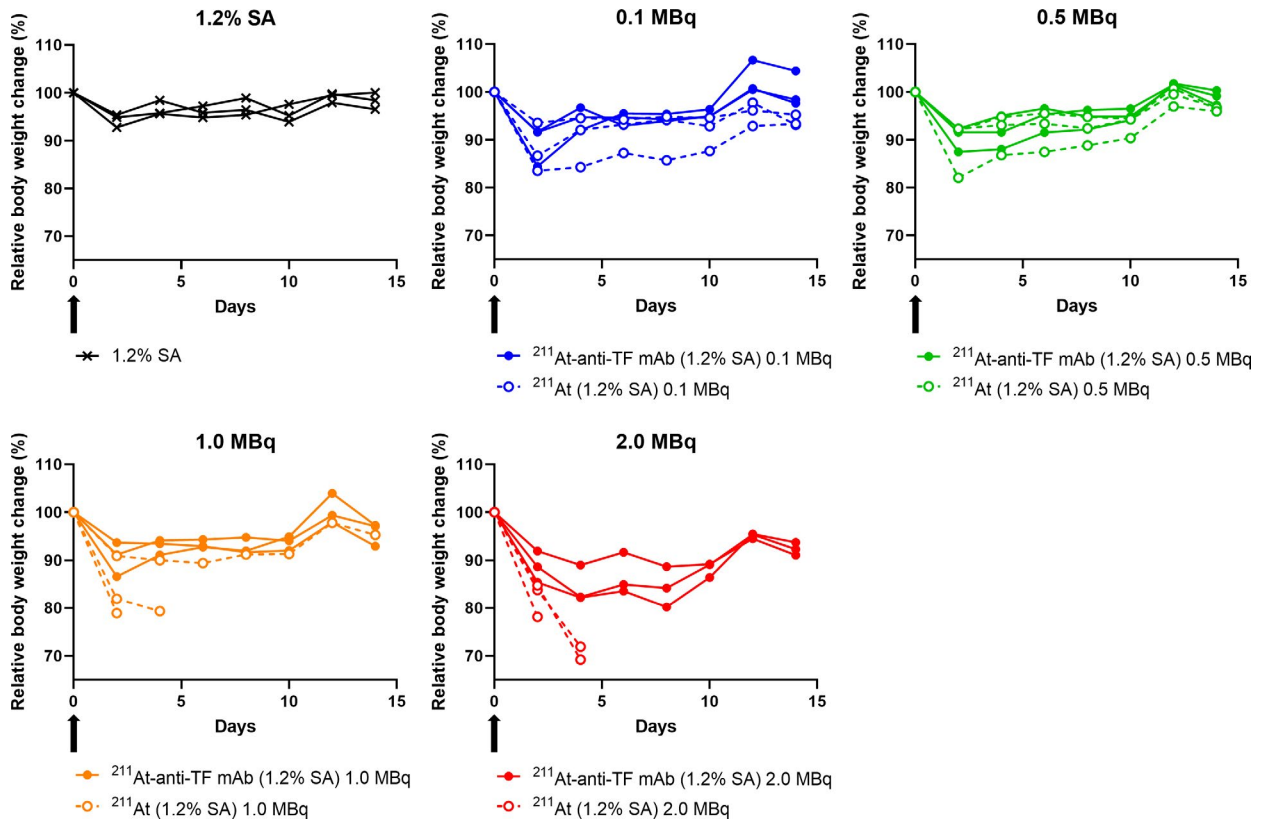


FIGURE 6 Toxicity of sodium ascorbate (SA), free astatine-211 (^{211}At), and ^{211}At -conjugated anti-tissue factor monoclonal antibody (^{211}At -anti-TF mAb). Arrows, injection; number of animals per each group, $n = 3$

unique armed antibody. Double-strand breaks generated by alpha particle-induced ionization of DNA are less repairable than single-strand breaks via more sparsely ionizing radiation.^{48,49} Moreover, it is well known that alpha particle radiation with high LET is not influenced by oxygen concentrations in the tumor, and hypoxia-induced radioresistance is minimal for the high-LET radiation.⁴⁸⁻⁵⁰ In fact, ^{211}At -conjugated anti-TF mAb protected by SA showed a potent antitumor effect in gastric cancer xenograft models dependent on the level of TF on the cell membrane (Figures 2 and 7B). Although the mode of action is not entirely clear, considering the cellular binding activities of ^{211}At -anti-TF mAbs in SA solutions against TF on the cell surface (Figures 2 and 4A,B), the antigen-antibody reaction seems to contribute to *in vitro* and *in vivo* antitumor effects (Figures 5A,B and 7B). Conversely, tumors treated with a single administration of ^{211}At -anti-TF mAb recurred (Figure 7B). Multiple administrations of the astatinated mAb may exert a long-lasting antitumor effect. However, in order to evaluate the antitumor activity and toxicity of multiple administrations, sufficient supply system of ^{211}At should be established to enable frequent production of the astatinated antibody. To date, various antibodies such as an anti-CD20 antibody for lymphoma,⁵¹ an anti-HER2 antibody for gastric cancer,⁵² an anti-frizzled homolog 10 antibody for synovial sarcoma,⁴⁴ an anti-CD38 antibody for multiple myeloma,⁵³ an anti-tenascin antibody for malignant gliomas,⁵⁴ and an anti-sodium-dependent phosphate-transport protein

2b (NaPi2b) bivalent antigen-binding fragment ($\text{F}[\text{ab}']_2$) for ovarian cancer^{55,56} have been applied to radioimmunotherapy (RIT) with ^{211}At . The present data reveal that in addition to these mAbs, anti-TF mAb may be available to ^{211}At -RIT for patients with TF-positive gastric cancer.

Although the MTD and dose-limiting toxicity after systemic administration of ^{211}At -labeled pharmaceuticals have not been clinically determined,⁵⁷ the MTD of radiopharmaceuticals labeled with an alpha emitter with a shorter half-life tend to be higher than those conjugated with radionuclide with a longer half-life in both pre-clinical and clinical settings.^{57,58} Considering the half-life of ^{211}At , 7.2 hours,³¹ it is presumed that radiopharmaceuticals will be prepared using ^{211}At at high radioactivity levels and administered at high doses. As the ^{211}At -induced radiochemical reaction disturbs the binding activity of astatinated radiopharmaceuticals depending on the radiation dose,^{32,33} protection from ^{211}At -induced antibody denaturation will become increasingly important in clinical settings. In the present study, we successfully demonstrated that SA protected an astatinated mAb from denaturation without intolerable side effects *in vivo* (Figures 3, 4A,B, 5A,B, 6 and 7A), which suggests the availability of the radioprotectant in clinical settings.

In conclusion, without intolerable side effects, SA protected the astatinated clone 1084 from ^{211}At -induced denaturation, which resulted in potent antitumor activities of the immunoconjugate. These

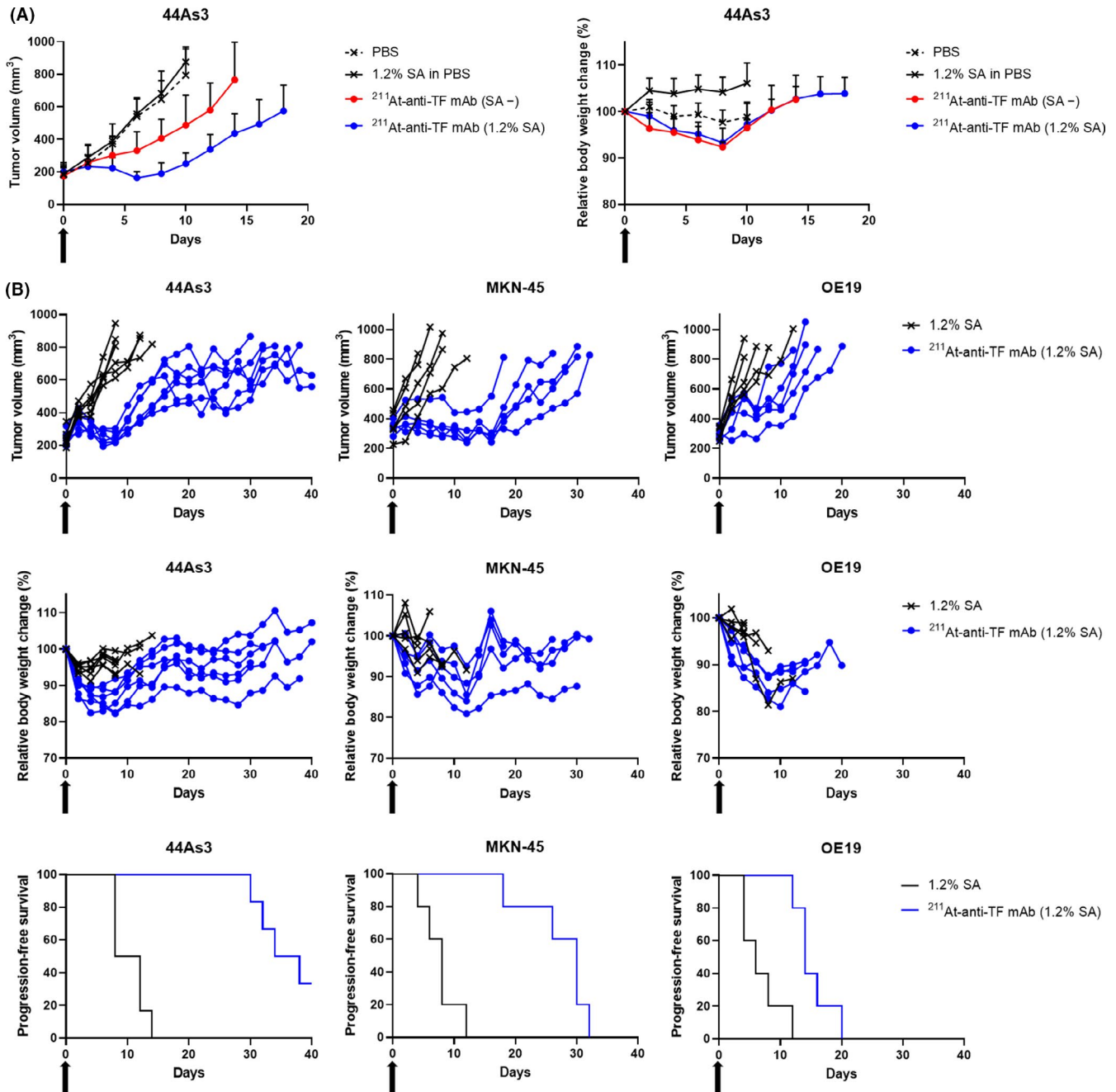


FIGURE 7 In vivo antitumor effect. A, The radioprotective effect of sodium ascorbate (SA) on antitumor activities of astatine-211-conjugated anti-tissue factor monoclonal antibody (²¹¹At-anti-TF mAb). Arrows, injection; points, mean; bars, standard deviation; number of animals per each group, $n = 5$. B, Antitumor effect and toxicity of ²¹¹At-anti-TF mAb in phosphate-buffered saline (PBS) containing 1.2% SA in the 44As3, MKN-45, and OE19 xenograft models. Number of animals per each group: 44As3, $n = 6$; MKN-45, $n = 5$; OE19, $n = 5$. Arrows indicate injection

findings suggest the clinical availability of the radioprotectant and applicability of clone 1084 to ²¹¹At-RIT.

ACKNOWLEDGMENTS

This work was supported by the Project for Cancer Research and Therapeutic Evolution (19cm0106237h0002 to H. Takashima) from the Japan Agency for Medical Research and Development (AMED), the National Cancer Center Research and Development Fund (29-A-9 to Y. Matsumura, 30-S-4 to Y. Koga, and 2020-A-9 to M. Yasunaga), and the

RIKEN Engineering Network Project (to S. Manabe). ²¹¹At was supplied through the Supply Platform of Short-lived Radioisotopes, supported by the JSPS Grant-in-Aid for Scientific Research on Innovative Areas (16H06278).

DISCLOSURE

Yasuhiro Matsumura is a cofounder, stockholder, and Board Member of RIN Institute Inc. Shino Manabe, Takahiro Anzai, and Masahiro Yasunaga are stockholders of RIN Institute Inc. Yasuhiro Matsumura

received research funds from RIN Institute Inc. The other authors declare no conflict of interest.

ORCID

Hiroki Takashima  <https://orcid.org/0000-0001-6487-7344>

Yoshikatsu Koga  <https://orcid.org/0000-0002-8404-585X>

Shino Manabe  <https://orcid.org/0000-0002-2763-1414>

Ryo Tsumura  <https://orcid.org/0000-0003-1732-9171>

Masahiro Yasunaga  <https://orcid.org/0000-0003-3356-0197>

REFERENCES

- Bray F, Ferlay J, Soerjomataram I, Siegel RL, Torre LA, Jemal A. Global cancer statistics 2018: GLOBOCAN estimates of incidence and mortality worldwide for 36 cancers in 185 countries. *CA Cancer J Clin*. 2018;68:394-424.
- Van Cutsem E, Sagaert X, Topal B, Haustermans K, Prenen H. Gastric cancer. *Lancet*. 2016;388:2654-2664.
- Bang YJ, Van Cutsem E, Feyereislova A, et al. Trastuzumab in combination with chemotherapy versus chemotherapy alone for treatment of HER2-positive advanced gastric or gastro-oesophageal junction cancer (ToGA): a phase 3, open-label, randomised controlled trial. *Lancet*. 2010;376:687-697.
- Shitara K, Iwata H, Takahashi S, et al. Trastuzumab deruxtecan (DS-8201a) in patients with advanced HER2-positive gastric cancer: a dose-expansion, phase 1 study. *Lancet Oncol*. 2019;20:827-836. <https://doi.org/10.1080/14712598.2020.1802423>
- Koganemaru S, Shitara K. Antibody-drug conjugates to treat gastric cancer. *Expert Opin Biol Ther*. 2020;1-8.
- Van Cutsem E, Bang YJ, Feng-Yi F, et al. HER2 screening data from ToGA: targeting HER2 in gastric and gastroesophageal junction cancer. *Gastric Cancer*. 2015;18:476-484.
- Mitani S, Kawakami H. Emerging targeted therapies for HER2 positive gastric cancer that can overcome trastuzumab resistance. *Cancers*. 2020;12:400.
- Stein PD, Beemath A, Meyers FA, Skaf E, Sanchez J, Olson RE. Incidence of venous thromboembolism in patients hospitalized with cancer. *Am J Med*. 2006;119:60-68.
- Bazan JF. Structural design and molecular evolution of a cytokine receptor superfamily. *Proc Natl Acad Sci USA*. 1990;87:6934-6938.
- van den Berg YW, Osanto S, Reitsma PH, Versteeg HH. The relationship between tissue factor and cancer progression: insights from bench and bedside. *Blood*. 2012;119:924-932.
- Yamashita H, Kitayama J, Ishikawa M, Nagawa H. Tissue factor expression is a clinical indicator of lymphatic metastasis and poor prognosis in gastric cancer with intestinal phenotype. *J Surg Oncol*. 2007;95:324-331.
- Geddings JE, Mackman N. Tumor-derived tissue factor-positive microparticles and venous thrombosis in cancer patients. *Blood*. 2013;122:1873-1880.
- Hisada Y, Mackman N. Cancer-associated pathways and biomarkers of venous thrombosis. *Blood*. 2017;130:1499-1506.
- Breij EC, de Goeij BE, Verploegen S, et al. An antibody-drug conjugate that targets tissue factor exhibits potent therapeutic activity against a broad range of solid tumors. *Cancer Res*. 2014;74:1214-1226.
- de Goeij BE, Satijn D, Freitag CM, et al. High turnover of tissue factor enables efficient intracellular delivery of antibody-drug conjugates. *Mol Cancer Ther*. 2015;14:1130-1140.
- Koga Y, Manabe S, Aihara Y, et al. Antitumor effect of antitissue factor antibody-MMAE conjugate in human pancreatic tumor xenografts. *Int J Cancer*. 2015;137:1457-1466.
- Zhang X, Li Q, Zhao H, et al. Pathological expression of tissue factor confers promising antitumor response to a novel therapeutic antibody SC1 in triple negative breast cancer and pancreatic adenocarcinoma. *Oncotarget*. 2017;8:59086-59102.
- Theunissen JW, Cai AG, Bhatti MM, et al. Treating tissue factor-positive cancers with antibody-drug conjugates that do not affect blood clotting. *Mol Cancer Ther*. 2018;17:2412-2426.
- Tsumura R, Manabe S, Takashima H, Koga Y, Yasunaga M, Matsumura Y. Influence of the dissociation rate constant on the intra-tumor distribution of antibody-drug conjugate against tissue factor. *J Control Release*. 2018;284:49-56.
- de Bono JS, Concin N, Hong DS, et al. Tisotumab vedotin in patients with advanced or metastatic solid tumours (InnovaTV 201): a first-in-human, multicentre, phase 1-2 trial. *Lancet Oncol*. 2019;20:383-393.
- Hong DS, Concin N, Vergote I, et al. Tisotumab vedotin in previously treated recurrent or metastatic cervical cancer. *Clin Cancer Res*. 2020;26:1220-1228.
- Aung W, Tsuji AB, Sugyo A, et al. Near-infrared photoimmunotherapy of pancreatic cancer using an indocyanine green-labeled anti-tissue factor antibody. *World J Gastroenterol*. 2018;24:5491-5504.
- Saito Y, Hashimoto Y, Kuroda J, et al. The inhibition of pancreatic cancer invasion-metastasis cascade in both cellular signal and blood coagulation cascade of tissue factor by its neutralisation antibody. *Eur J Cancer*. 2011;47:2230-2239.
- Tsumura R, Sato R, Furuya F, et al. Feasibility study of the Fab fragment of a monoclonal antibody against tissue factor as a diagnostic tool. *Int J Oncol*. 2015;47:2107-2114.
- Yamamoto Y, Hyodo I, Koga Y, et al. Enhanced antitumor effect of anti-tissue factor antibody-conjugated epirubicin-incorporating micelles in xenograft models. *Cancer Sci*. 2015;106:627-634.
- Sugaya A, Hyodo I, Koga Y, et al. Utility of epirubicin-incorporating micelles tagged with anti-tissue factor antibody clone with no anti-coagulant effect. *Cancer Sci*. 2016;107:335-340.
- Takashima H, Tsuji AB, Saga T, et al. Molecular imaging using an anti-human tissue factor monoclonal antibody in an orthotopic glioma xenograft model. *Sci Rep*. 2017;7:12341.
- Sugyo A, Aung W, Tsuji AB, et al. Antitissue factor antibody-mediated immunoSPECT imaging of tissue factor expression in mouse models of pancreatic cancer. *Oncol Rep*. 2019;41:2371-2378.
- Takashima H, Koga Y, Tsumura R, et al. Reinforcement of antitumor effect of micelles containing anticancer drugs by binding of an anti-tissue factor antibody without direct cytotoxic effects. *J Control Release*. 2020;323:138-150.
- Aghevlian S, Boyle AJ, Reilly RM. Radioimmunotherapy of cancer with high linear energy transfer (LET) radiation delivered by radionuclides emitting α -particles or Auger electrons. *Adv Drug Deliv Rev*. 2017;109:102-118.
- Zalutsky MR, Pruszyński M. Astatine-211: production and availability. *Curr Radiopharm*. 2011;4:177-185.
- Larsen RH, Bruland ØS. Radiolysis of radioimmunoconjugates. Reduction in antigen-binding ability by α -particle radiation. *J Labelled Compd Radiopharm*. 1995;36:1009-1018.
- Zalutsky MR, Zhao XG, Alston KL, Bigner D. High-level production of alpha-particle-emitting (211)At and preparation of (211)At-labeled antibodies for clinical use. *J Nucl Med*. 2001;42:1508-1515.
- Yanagihara K, Takigahira M, Tanaka H, et al. Development and biological analysis of peritoneal metastasis mouse models for human scirrhous stomach cancer. *Cancer Sci*. 2005;96:323-332.
- Yanagihara K, Takigahira M, Takeshita F, et al. A photon counting technique for quantitatively evaluating progression of peritoneal tumor dissemination. *Cancer Res*. 2006;66:7532-7539.
- Yamamoto Y, Hyodo I, Takigahira M, et al. Effect of combined treatment with the epirubicin-incorporating micelles (NC-6300) and 1,2-diaminocyclohexane platinum (II)-incorporating micelles (NC-4016) on a human gastric cancer model. *Int J Cancer*. 2014;135:214-223.

37. Sajjad M, Riaz U, Yao R, et al. Investigation of 3'-debenzoyl-3'-(3-([¹²⁴I]-iodobenzoyl))paclitaxel analog as a radio-tracer to study multi-drug resistance in vivo. *Appl Radiat Isot.* 2012;70:1624-1631.
38. Fuchigami H, Manabe S, Yasunaga M, Matsumura Y. Chemotherapy payload of anti-insoluble fibrin antibody-drug conjugate is released specifically upon binding to fibrin. *Sci Rep.* 2018;8:14211.
39. Lindegren S, Frost S, Back T, Haglund E, Elgqvist J, Jensen H. Direct procedure for the production of ²¹¹At-labeled antibodies with an epsilon-lysyl-3-(trimethylstannyl)benzamide immunoconjugate. *J Nucl Med.* 2008;49:1537-1545.
40. Aneheim E, Gustafsson A, Albertsson P, et al. Synthesis and evaluation of astatinated N-[2-(Maleimido)ethyl]-3-(trimethylstannyl) benzamide immunoconjugates. *Bioconjug Chem.* 2016;27:688-697.
41. Shoemaker AR, Mitten MJ, Adickes J, et al. Activity of the Bcl-2 family inhibitor ABT-263 in a panel of small cell lung cancer xenograft models. *Clin Cancer Res.* 2008;14:3268-3277.
42. McDevitt MR, Finn RD, Ma D, Larson SM, Scheinberg DA. Preparation of alpha-emitting ²¹³Bi-labeled antibody constructs for clinical use. *J Nucl Med.* 1999;40:1722-1727.
43. Tsumura R, Anzai T, Manabe S, et al. Antitumor effect of humanized anti-tissue factor antibody-drug conjugate in a model of peritoneal disseminated pancreatic cancer. *Oncol Rep.* 2021;45:329-336.
44. Li HK, Sugyo A, Tsuji AB, et al. α -particle therapy for synovial sarcoma in the mouse using an astatine-211-labeled antibody against frizzled homolog 10. *Cancer Sci.* 2018;109:2302-2309.
45. Robinson MK, Shaller C, Garmestani K, et al. Effective treatment of established human breast tumor xenografts in immunodeficient mice with a single dose of the alpha-emitting radioisotope astatine-211 conjugated to anti-HER2/neu diabodies. *Clin Cancer Res.* 2008;14:875-882.
46. Hong H, Zhang Y, Nayak TR, et al. Immuno-PET of tissue factor in pancreatic cancer. *J Nucl Med.* 2012;53:1748-1754.
47. Shi S, Hong H, Orbay H, et al. ImmunoPET of tissue factor expression in triple-negative breast cancer with a radiolabeled antibody Fab fragment. *Eur J Nucl Med Mol Imaging.* 2015;42:1295-1303.
48. Kassis AI, Adelstein SJ. Radiobiologic principles in radionuclide therapy. *J Nucl Med.* 2005;46(Suppl 1):4s-12s.
49. Kassis AI. Therapeutic radionuclides: biophysical and radiobiologic principles. *Semin Nucl Med.* 2008;38:358-366.
50. Sgouros G, Roeske JC, McDevitt MR, et al. MIRD Pamphlet No. 22 (abridged): radiobiology and dosimetry of alpha-particle emitters for targeted radionuclide therapy. *J Nucl Med.* 2010;51:311-328.
51. Green DJ, Shadman M, Jones JC, et al. Astatine-211 conjugated to an anti-CD20 monoclonal antibody eradicates disseminated B-cell lymphoma in a mouse model. *Blood.* 2015;125:2111-2119.
52. Li HK, Morokoshi Y, Nagatsu K, Kamada T, Hasegawa S. Locoregional therapy with α -emitting trastuzumab against peritoneal metastasis of human epidermal growth factor receptor 2-positive gastric cancer in mice. *Cancer Sci.* 2017;108:1648-1656.
53. O'Steen S, Comstock ML, Orozco JJ, et al. The α -emitter astatine-211 targeted to CD38 can eradicate multiple myeloma in a disseminated disease model. *Blood.* 2019;134:1247-1256.
54. Zalutsky MR, Reardon DA, Akabani G, et al. Clinical experience with alpha-particle emitting ²¹¹At: treatment of recurrent brain tumor patients with ²¹¹At-labeled chimeric antitenascin monoclonal antibody 81C6. *J Nucl Med.* 2008;49:30-38.
55. Bäck T, Chouin N, Lindegren S, et al. Cure of human ovarian carcinoma solid xenografts by fractionated α -Radioimmunotherapy with (²¹¹At)-MX35-F(ab')(2): influence of absorbed tumor dose and effect on long-term survival. *J Nucl Med.* 2017;58:598-604.
56. Hallqvist A, Bergmark K, Bäck T, et al. Intraperitoneal α -emitting radioimmunotherapy with (²¹¹At) in relapsed ovarian cancer: long-term follow-up with individual absorbed dose estimations. *J Nucl Med.* 2019;60:1073-1079.
57. Makvandi M, Dupis E, Engle JW, et al. Alpha-emitters and targeted alpha therapy in oncology: from basic science to clinical investigations. *Target Oncol.* 2018;13:189-203.
58. Poty S, Francesconi LC, McDevitt MR, Morris MJ, Lewis JS. α -Emitters for radiotherapy: from basic radiochemistry to clinical studies-part 2. *J Nucl Med.* 2018;59:1020-1027.

SUPPORTING INFORMATION

Additional supporting information may be found online in the Supporting Information section.

How to cite this article: Takashima H, Koga Y, Manabe S, et al. Radioimmunotherapy with an ²¹¹At-labeled anti-tissue factor antibody protected by sodium ascorbate. *Cancer Sci.* 2021;112:1975-1986. <https://doi.org/10.1111/cas.14857>